Second Moment of the Cr^{3+} EPR Line in Ruby Broadened by Strong Hyperfine Interactions

RICHARD F. WENZEL
Naval Research Laboratory, Washington, D. C. 20390
(Received 13 June 1969; revised manuscript received 15 December 1969)

An alternative approach to the Van Vleck formalism for calculating the second moment of an EPR line in the case of strong (super) hyperfine interactions is described. The calculation uses probability theory to arrive at the following expression for the second moment of the EPR line:

$$\langle \Delta E^2 \rangle = (2I+1)^{-1} \sum_{i=1}^{N} \sum_{j=1}^{2I+1} \sum_{k=1}^{2I+1} [\epsilon_a(j_i) - \epsilon_b(k_i)]^2 \cdot P_i(j,k),$$

where $\epsilon_a(j_i)$ and $\epsilon_b(k_i)$ are the exact energy levels of the ith nucleus in the presence of the paramagnetic ion, when the ion is in its j_ith initial and k_ith final state, respectively, and I is the spin of the nucleus. The $P_i(j,k)$ are the "transition" probabilities for the ith nucleus in the j_ith level of the initial spin states to be found in the k_ith level of the final nuclear-spin states after the ion transition. The paramagnetic ion strongly interacts with N nuclear spins. The anisotropic EPR-line width variation of dilute Verneuil ruby has been analyzed, using this formulation, in terms of the (super) hyperfine interaction with the surrounding aluminum nuclei. The calculation shows that most of the linewidth (70 to 80%) is caused by the hyperfine interaction. The line shape is also calculated by a Monte Carlo technique and is found to be Gaussian.

I. INTRODUCTION

THE second moment of an EPR line in the case of strong spin-spin interaction was originally obtained by Van Vleck.[1] The results of the calculation are often employed in the case of the broadening of the EPR line of a dilute paramagnetic ion by nuclear (super) hyperfine interactions.[2,3] When so used, care must be taken that the conditions applicable to the Van Vleck calculation are satisfied. It is the purpose of this paper to point out an alternate approach to the Van Vleck formalism in the nuclear hyperfine case, which appears to display more explicitly the mechanisms operative and to allow the calculation of more complex cases.

This work will report a calculation of the second moment for the case of the broadening of a dilute paramagnetic-ion EPR line by strong nuclear hyperfine interaction and the application of this technique to the EPR linewidth of the Cr^{3+} ion in dilute ruby. The second moment calculated using this technique will be compared with the second moment obtained by generating the line shape by a Monte Carlo calculation.

II. SECOND-MOMENT CALCULATION

The case considered is the one in which the paramagnetic ion may have strong (super) hyperfine interaction with surrounding paramagnetic nuclei.

The Hamiltonian of the total spin system (paramagnetic ion and all paramagnetic nuclei) is

$$\mathcal{H} = g\beta \mathbf{S}\cdot\mathbf{H} + D[S_z^2 - \tfrac{1}{3}S(S+1)] + \sum_{i=1}^{i=N} [A_i \mathbf{S}\cdot\mathbf{I} + B_i(\mathbf{S}\cdot\mathbf{n}_i)(\mathbf{I}_i\cdot\hat{\mathbf{n}}_i) - \gamma/I(\mathbf{I}_i\cdot\mathbf{H}) + Q_i I_{zi}^2], \quad (1)$$

where A_i and B_i are appropriate combinations of the hyperfine and contact-interaction coupling constants, Q_i the quadrupole moment, and γ the nuclear moment of the ith nucleus. The Hamiltonian given by Eq. (1) is specialized to the case applicable to the Cr^{3+} ion in Al_2O_3 (ruby), but additional fine-structure terms may be added without effecting the subsequent arguments. The vector $\hat{\mathbf{n}}$ is a unit vector from the paramagnetic ion to the ith nuclear site. The paramagnetic ion is considered to be very dilute in the lattice, and, consequently, the spin-spin interaction between the ions is neglected. A treatment of the problem of spin-spin interaction has been done by Grant and is given in Refs. 4–7.

The Hamiltonian given by Eq. (1) will be divided into two parts, those terms involving only operators that apply to the paramagnetic ion, and all other terms. The paramagnetic-ion Hamiltonian can be solved by conventional techniques obtaining a set of eigenfunctions and energy eigenvalues that describe the isolated ion. The part of the Hamiltonian involving the nuclei and their interaction with the ion can be solved by employing two approximations.

[1] J. H. Van Vleck, Phys. Rev. **74**, 1168 (1948).
[2] N. Laurance, E. C. McIrvine, and J. Lambe, J. Phys. Chem. Solids **23**, 515 (1962).
[3] W. J. C. Grant and M. W. P. Strandberg, Phys. Rev. **135**, A737 (1964).
[4] W. J. C. Grant and M. W. P. Strandberg, Phys. Rev. **135**, A724 (1964).
[5] W. J. C. Grant, Phys. Rev. **134**, A1554 (1964); **134**, A1565 (1964); **134**, A1574 (1964).
[6] W. J. C. Grant, Phys. Rev. **135**, A1265 (1964).
[7] W. J. C. Grant, Physica **30**, 1433 (1964).

First, it is assumed that the nuclei have a negligible effect on the expectation values of the ion-spin operators $\langle S_x\rangle$, $\langle S_y\rangle$, and $\langle S_z\rangle$. Second, the nuclei do not strongly interact with one another. Both of these assumptions are generally valid and will be found to be valid in the case of ruby. Under these conditions, the energy levels of Eq. (1) can be obtained by solving the individual *nuclear* Hamiltonians, using the expectation values of the ion-spin operators to replace the operators. This calculates the average instantaneous local magnetic field at the site of the nuclei caused by the paramagnetic ion. The total energy of the system will then be given by the sum of the paramagnetic-ion energy and of the several nuclear energies.

An individual nuclear Hamiltonian is, for the ith nucleus,

$$\mathcal{H}'=A_i\langle\mathbf{S}\rangle\cdot\mathbf{I}_i+B_i(\langle\mathbf{S}\rangle\cdot\hat{\mathbf{n}}_i)(\mathbf{I}_i\cdot\hat{\mathbf{n}}_i)+\gamma/I(\mathbf{I}_i\cdot\mathbf{H})+Q_iI_{zi}^2. \quad (2)$$

Since strong (super) hyperfine interactions are to be included, Eq. (2) must in general be solved exactly by computer methods since the hyperfine term may be of the same order as the nuclear Zeeman term.

The exact solution of Eq. (2) results in a set of energy eigenvalues and eigenfunctions for the ith nucleus. However, the EPR transition of the paramagnetic ion takes place between two different spin levels of the ion that will have two different values of $\langle\mathbf{S}\rangle$. Consequently, there will be two nuclear Hamiltonians to solve, one for the initial- and one for the final-spin state. The two sets of nuclear eigenvalues and eigenfunctions of Eq. (2) for the initial and final states will be labeled ϵ_a, Ψ_a, ϵ_b, and Ψ_b, respectively.

The energy levels of Eq. (1) are then, in the approximations mentioned above,

$$E_a=g\beta\langle\mathbf{S}\rangle_a\cdot\mathbf{H}+D[\langle S_z^2\rangle_a-\tfrac{1}{3}S(S+1)]+\sum_{i=1}^{i=N}\epsilon_a(j_i), \quad (3)$$

where j_i indicates that the ith nucleus is in the jth nuclear-energy level. In the following, it will be understood that a sum or product over i is from $i=1$ to $i=N$; a sum over j and k will be from $j=1$ to $j=2I+1$, $k=1$ to $k=2I+1$. A similar energy E_b can be obtained for the final paramagnetic-ion state. The total change in energy for the entire system in an EPR transition is

$$E_a-E_b=g\beta(\langle\mathbf{S}\rangle_a-\langle\mathbf{S}\rangle_b)\cdot\mathbf{H}+D(\langle S_z^2\rangle_a-\langle S_z^2\rangle_b)+\sum_i[\epsilon_a(j_i)-\epsilon_b(k_i)], \quad (4)$$

where k_i indicates that the ith nucleus is found in the kth eigenstate after the ion transition. The terms involving $\langle\mathbf{S}\rangle$ pertain to the EPR transition in the absence of the hyperfine interaction and will be the same for any arrangement of the nuclear spins under the assumptions employed. Consequently, this constant energy difference will be subtracted in all that follows. Thus,

$$\Delta E=\sum_i[\epsilon_a(j_i)-\epsilon_b(k_i)]. \quad (5)$$

In the usual EPR experiment, only the paramagnetic ion makes a transition. Assume before the transition that the ith nucleus is in the jth nuclear state. The probability that this will occur is

$$P_i(j)\equiv(2I+1)^{-1} \quad (6)$$

since all levels are equally probable[8] (in the high-temperature approximation). After the ion transition, the wave function of the nuclear state $\Psi_a(j_i)$ has not changed but must now be expressed in terms of the new nuclear wave function appropriate after the nuclear transition $\Psi_b(k_i)$.[9] The probability that, given the ith nucleus was in the j_ith state before an ion transition, it will be found in the k_jth state after a transition is defined as the conditional probability

$$P_i(j,k)\equiv|\langle\Psi_a(j_i)|\Psi_b(k_i)\rangle|^2. \quad (7)$$

Some properties of the $P_i(j,k)$ are

$$\sum_j P_i(j,k)=\sum_k P_i(j,k)=1. \quad (8)$$

The probability that the whole spin system will change by an energy ΔE is

$$P(\Delta E)=\int_{-\infty}^{+\infty}d\rho\,\exp\{i\rho[\Delta E-\sum_i[\epsilon_a(j_i)-\epsilon_b(k_i)]]\}\times\prod_j P_i(j_i)\prod_k P_i(j,k), \quad (9)$$

where the integral expression for the delta function has been employed to choose those particular combinations of j_i and k_i that give an energy ΔE. Since j_i and k_i are discrete, $P(\Delta E)$ is a discrete distribution. The second moment of ΔE is defined as

$$\langle\Delta E^2\rangle=\sum(\Delta E)^2P(\Delta E)[\sum P(\Delta E)]^{-1}, \quad (10)$$

where the summation in Eq. (10) is over all possible combinations of initial and final nuclear states of all N nuclei. Such a summation will be indicated in the following by a summation sign with no subscript.

The denominator in Eq. (10) can be evaluated by noting that it is Eq. (9) summed over all possible combinations of initial and final nuclear states. Each possible combination of states is counted once, and the total number of terms in the sum is $(2I+1)^{2N}$, there being $(2I+1)^2$ choices of initial and final states for each of N nuclei. Selecting from this sum the terms in which a prescribed N-1 of the nuclei have fixed initial and final states, i.e., $j_1=3$, $k_1=5$, $j_2=4$, $k_2=7$, etc., the

[8] C. P. Slichter, in *Principles of Magnetic Resonance* (Harper & Row Publishers, Inc., New York, 1963), p. 235.

[9] C. P. Slichter, in *Principles of Magentic Resonance* (Harper & Row Publishers, Inc., New York, 1963), p. 195.

result is a sum only on the i_0th chosen nucleus. Since all possible combinations of quantum numbers are represented in the total sum, the chosen terms involving the i_0th nucleus are just the sum over the possible initial and final states of the i_0th nucleus. This sum is written

$$\text{partial sum}=a\sum_j[P_i(j_i)\sum_k P_i(j,k)], \quad (11)$$

where a is a constant. Employing Eq. (8), Eq. (11) becomes

$$\text{partial sum}=a\sum_i P(j_i)=a(2I+1)^{-1}(2I+1)=a. \quad (12)$$

This can similarly be done for all other possible combinations of fixed initial and final states of the other N-1 nuclei. This grouping will then include all the terms of the sum. When this is done, all probabilities involving the i_0th nucleus will have been summed, and these will sum to one. Likewise, the remaining terms can be grouped to sum over all the states of each other nucleus in turn. The denominator of Eq. (10) is then

$$\sum P(\Delta E)=1, \quad (13)$$

and the probability distribution is normalized to 1. Equation (10) becomes

$$\langle\Delta E^2\rangle=\sum(\Delta E^2)\int_{-\infty}^{+\infty}d\rho \times\exp(i\rho\{\Delta E-\sum_i[\epsilon_a(j_i)-\epsilon_b(k_i)]\}) \times\prod_j P_i(j_i)\prod_k P_i(j,k). \quad (14)$$

The integral over ρ can be performed, resulting in

$$\langle\Delta E^2\rangle=\sum(\sum_i[\epsilon_a(j_i)-\epsilon_b(k_i)])^2\prod_j P_i(j_i)\prod_k P_i(j,k). \quad (15)$$

The squared expression in Eq. (15) contains all crossproducts of the i nuclei. A typical cross term in the sum is, for the sth and pth nuclei,

$$[\epsilon_a(j_s)-\epsilon_b(k_s)][\epsilon_a(j_p)-\epsilon_b(k_p)] \times\prod_j P_i(j_i)\prod_k P_i(j,k). \quad (16)$$

Considering all terms in the sum over all possible states of this type, the probabilities not explicitly involving the sth and pth nuclei sum to 1, leaving

$$\sum_{jp}\sum_{kp}\sum_{js}\sum_{ks}[\epsilon_a(j_p)-\epsilon_b(k_p)][\epsilon_a(j_s)-\epsilon_b(k_s)] \times P_s(j_s)P_s(j,k)P_p(j_p)P_p(j,k). \quad (17)$$

The terms $P_s(j_s)$ and $P_p(j_p)$ are both $(2I+1)^{-1}$.

The $\epsilon_a(j_s)$ and $\epsilon_b(k_s)$ are the initial- and final-energy eigenvalues for the sth nucleus. If the quadrupole term in the nuclear Hamiltonian [Eq. (2)] is chosen to be traceless, then

$$\sum_j\epsilon_a(j_s)=\sum_k\epsilon_b(k_s)=0, \quad (18)$$

or, if the quadrupole term is not chosen to be traceless,

$$\sum_j\epsilon_a(j_s)-\sum_k\epsilon_b(k_s)=0. \quad (19)$$

Consider all the terms in the sum for which the pth nucleus has a fixed initial and final state. Equation (17) is then

$$B(2I+1)^{-2}(\sum_j\epsilon_a(j_s)\sum_k P_s(j,k) -\sum_k\epsilon_b(k_s)\sum_j P_s(j,k)), \quad (20)$$

where B is a constant, which by Eq. (8) becomes

$$B(2I+1)^{-2}(\sum_j\epsilon_a(j_s)-\sum_k\epsilon_b(k_s))=0 \quad (21)$$

because of Eqs. (18) or (19).

Thus, the cross term chosen is zero for this term, and all other terms in the p sum. Since Eq. (17) is general, all cross-product terms are zero. Thus, only the squares of the individual terms in Eq. (15) contribute to the second moment. Equation (15) becomes

$$\langle\Delta E^2\rangle=\sum(\sum_i[\epsilon_a(j_i)-\epsilon_b(k_i)]^2 \times\prod_j P_i(j_i)\prod_k P_i(j,k)). \quad (22)$$

Consider all the terms in this sum for the rth nucleus, in which the initial and final states are q and t, respectively. The probabilities involving the other N-1 nuclei will each sum to one in the sum over all possible states with q and t fixed for the rth nucleus. This will also occur for all the other possible initial and final states for the rth nucleus. The same procedure can be repeated for every other nucleus, obtaining for the second moment

$$\langle\Delta E^2\rangle=\sum_i\sum_j\sum_k[\epsilon_a(j_i)-\epsilon_b(k_i)]P_i(j_i)P_i(j,k), \quad (23)$$

but $P_i(j_i)=(2I+1)^{-1}$. So, finally,

$$\langle\Delta E^2\rangle=(2I+1)^{-1}\sum_i\sum_j\sum_k[\epsilon_a(j_i)-\epsilon_b(k_i)]P_i(j,k). \quad (24)$$

The second moment is thus the sum of the squares of the possible individual transitions weighted by their respective conditional probabilities and divided by $2I+1$.

Equation (24) can be reduced somewhat further by expanding the squared terms and noting that the

TABLE I. The (super) hyperfine coupling constants obtained from Ref. 13, written in the notation of Eq. (4) for the first-13 aluminum nearest neighbors.

Site number	A (MHz)	B (MHz)	Q (MHz)
1	−0.32	3.0	0.265
2, 3, 4	2.32	2.76	0.14
5, 6, 7	1.58	1.89	0.145
8, 9, 10	1.91	1.42	0.17
11, 12, 13	0.85	1.42	0.175

summations on the squared terms are just the respective traces.

$$\langle \Delta E^2 \rangle = (2I+1)^{-1} \sum_i [\mathrm{Tr}(\mathcal{H}_{ia}'^2) + \mathrm{Tr}(\mathcal{H}_{ib}'^2) - 2 \sum_j \sum_k \epsilon_a(j_i)\epsilon_b(k_i) P_i(j,k)], \quad (25)$$

where Tr signifies the trace. This can be reduced no further, and it is still necessary to know the ϵ_a, ϵ_b, and $P_i(j,k)$ in order to calculate the cross term.

The calculation of the second moment reduces, then, to the problem of the calculation of the exact energy levels of the nuclei and the transition probabilities.

For nuclei that have only slight interaction with the ion, the nuclei will be quantized along the direction of the magnetic field. However, for paramagnetic ions with significant fine structure, $\langle \mathbf{S} \rangle$ is rarely along the direction of the magnetic field, and the Van Vleck result does not hold without modification. However, in that case, the ϵ_a and ϵ_b can be readily calculated, and the $P_i(j,k) = \delta_{jk}$. If $\hat{h}$ is the direction of the magnetic field, the second moment becomes

$$\langle \Delta E^2 \rangle = \tfrac{1}{3} I(I+1) \sum_i [A_i(\langle S_h \rangle_a - \langle S_h \rangle_b) + B_i(\langle \mathbf{S} \rangle_a - \langle \mathbf{S} \rangle_b) \cdot \hat{\mathbf{n}} n_h]^2, \quad (26)$$

where n_h is the component of $\hat{\mathbf{n}}$ along the magnetic-field direction. This approximation will be useful in the following sections.

III. EPR LINEWIDTH IN RUBY

The angular variation of the EPR Cr^{3+} linewidth in ruby has been reported by several authors.[10–12] Curtis *et al.*[10] analyzed the angular variation of vapor-phase rubies at 35 GHz in terms of mosaic imperfections. Kirkby and Thorp[11] analyzed vapor-phase, Verneuil, and Czochralski rubies at 35 GHz in terms of a mosaic misorientation and strains. Wenzel and Kim,[12] hereafter referred to as WK, also analyzed the angular variation in dilute Verneuil ruby in terms of mosaic misorientation and strains.

[10] D. A. Curtis, C. J. Kirkby, and J. S. Thorp, Brit. J. Appl. Phys. **16**, 1681 (1965).
[11] C. J. Kirkby and J. S. Thorp, Proc. Phys. Soc. (London) **C1**, 913 (1968).
[12] R. F. Wenzel and Y. W. Kim, Phys. Rev. **140**, A1592 (1965).

The analysis by WK demonstrated that mosaic misorientation and strains could not account for the angular variation, and a different broadening mechanism was probably operative, at least in the case of very small samples of dilute Verneuil ruby.

The line shape observed by WK was quite closely Gaussian for all transitions and angles. The same linewidth and angular variation was found for two small samples (3-mm cubes) from two different boules and with chromium concentrations varying by a factor of 10 (0.001 and 0.01%). This suggests that the cause of the anisotropic linewidth broadening is not a defect property of the crystal but is inherent to the spin system itself. Such an inherent mechanism will be examined in the following and shown to account for the majority of the observed anisotropic broadening. This mechanism is the hyperfine interaction of the Cr^{3+} ion with the surrounding aluminum nuclei.

In spin systems in which there are significant (super) hyperfine interactions between the paramagnetic ion and surrounding paramagnetic nuclei, sizeable anisotropic broadening of the EPR transition may occur. The second moment of the EPR line under these conditions is given by Eq. (24).

Equation (24) may be used to calculate the contribution to the second moment from all aluminum nuclei in the lattice. However, the calculation need only be carried out over the nuclei that strongly interact with the Cr^{3+} ion. Equation (26), a modified form of the Van Vleck second-moment expression for unlike spins, can be employed for more distance nuclei.

In the case of ruby, Cr^{3+} in Al_2O_3, the aluminum nuclei have spin $I = \frac{5}{2}$, and are 100% abundant. The spin of the Cr^{3+} is $\frac{3}{2}$, and the spin Hamiltonian is

$$\mathcal{H} = g\beta \mathbf{S} \cdot \mathbf{H} + D[S_z^2 - \tfrac{1}{3} S(S+1)], \quad (27)$$

where g is 1.985 and D is −5.75 GHz. The aluminum nuclear-spin Hamiltonian is given by Eq. (2).

The Cr^{3+} is known to have strong (super) hyperfine interactions with the surrounding 13 aluminum nuclei.[2] The coefficients A and B in Eq. (2) are calculated from the data of Ref. 2 for these 13 nuclei and are given in Table I. The nuclear magnetic moment of the Al^{3+} ion γ is 3.6385 μ_n.

The eigenvalues and eigenfunctions of Eq. (27) for the Cr^{3+} ion alone can be calculated by computer techniques. This yields the $\langle \mathbf{S} \rangle_a$ and $\langle \mathbf{S} \rangle_b$ for the initial and final Cr^{3+} levels, respectively, of the ion EPR transition alone. The expectation values $\langle \mathbf{S} \rangle$ are then substituted into the Hamiltonian of Eq. (2) for an individual nuclear spin, and the Hamiltonian is solved exactly. An exact solution is necessary since the nuclear Zeeman term is of the same order as the hyperfine term. This yields the initial set of nuclear states of the jth nucleus $\epsilon_a(j_i)$ when $\langle \mathbf{S}_a \rangle$ is used in Eq. (2) and the final set $\epsilon_b(k_i)$ when $\langle \mathbf{S}_b \rangle$ is employed. The $\Psi_a(j_i)$ and $\Psi_b(k_i)$ of Eq. (24) are the eigenfunctions of Eq. (2), and, consequently, $P_i(j,k)$ can be calculated.

The contribution to the second moment from each of the 13 aluminum nuclei is obtained, and the total second moment is obtained by summing the 13 nuclei.

To compare this second moment, which is expressed in energy units (MHz^2) in terms of experimentally measured widths, it is also necessary to know dE/dH for the ion transition at the resonant magnetic field. This is given by

$$dE/dH = g\beta(\langle S_{za}\rangle - \langle S_{zb}\rangle)\cos\theta + g\beta(\langle S_{xa}\rangle - \langle S_{xb}\rangle)\sin\theta, \quad (28)$$

where θ is the angle between the C axis and the magnetic field, which can be readily calculated. For simplicity, it is assumed that the magnetic field is in the x-z plane. Finally, the square root of the second moment of a Gaussian line is equal to half the peak-to-peak (derivative) width of the EPR line.

The calculation outlined above has been done for several of the resonance lines observed at 9.4 GHz. Figure 1 shows the calculated peak-to-peak (derivative) width in gauss (solid circles). The experimental data of Ref. 12 for the 0.01% Cr^{3+} sample are also shown (triangles). The notation a, b, and c labels the $1 \rightarrow 2$, $1 \rightarrow 3LF$(low-field), and $3 \rightarrow 4$ transitions, respectively, in the notation given in Ref. 12.

Also shown on Fig. 1 is the linewidth (squares) predicted by the Van Vleck formulation when the nuclear spins, but not the spin of the ion, are assumed to be quantized along the direction of the magnetic field [see Eq. (26)].

IV. DISCUSSION

The angular variation predicted by the second-moment calculation is very similar to the experimentally observed variation, but is about 20 to 30% smaller in magnitude than the observed variation.

The linewidth calculated by the Van Vleck method [Eq. (26)], using the data of Ref. 2, greatly underestimates the linewidth. This calculation assumes that the Cr^{3+} spin is not along the magnetic field, but that the nuclear spins are so aligned. As can be seen from the figure, the effect of the ion on the nuclear spins is a major cause of the broadening.

However, Eq. (26) will result in nearly the correct linewidth when $\theta = 0°$ (see Ref. 2, pp. 539) since for this orientation $\langle \mathbf{S} \rangle$ is aligned along the magnetic field, and $\langle \mathbf{I} \rangle$ is very nearly so.

This analysis of the linewidth in dilute ruby is based upon a calculation of the second moment of the EPR line. Objections to using moment calculations to predict linewidth have been raised.[3–7] However, once the $\epsilon_a(j_i)$, $\epsilon_b(k_i)$, and the $P_i(j,k)$ are known for all relevant nuclei, it is possible to predict the *line shape* by a Monte Carlo calculation.

A Monte Carlo calculation consists of sampling a sufficient number of possible energy differences ΔE.

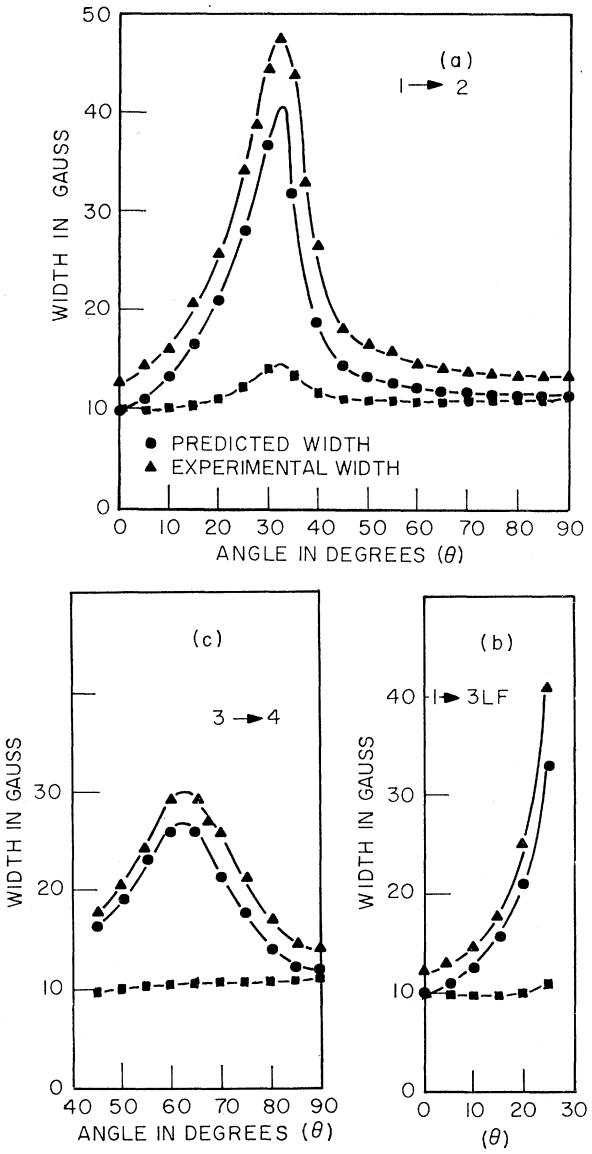

FIG. 1. Predicted and experimental EPR linewidth. The experimental EPR peak-to-peak width at 9.4 GHz for a 0.01% Cr sample of ruby as a function of the angle that the magnetic field makes with the crystallographic C axis is indicated by the triangles in the figures. The linewidth calculated by the mechanism of strong hyperfine interaction with the first-13 Al nuclei is indicated by the dots in the figures. The linewidth calculated using the modified Van Vleck formulation given by Eq. (26) is indicated by the squares. The three graphs, a, b, and c refer to three different EPR transitions in ruby at 9.4 GHz. (See Ref. 3 for the nomenclature.)

The discrete distribution of $P(\Delta E)$ can then be examined to determine the shape of the line.

The generation of a single ΔE is accomplished by assigning initial states j_i to all of the 13 nuclei. Since each initial state is equally probable (high-temperature approximation), a number is generated randomly between 1 and 6 (there are six possible initial states) in order to choose j_i. The initial states are thus chosen

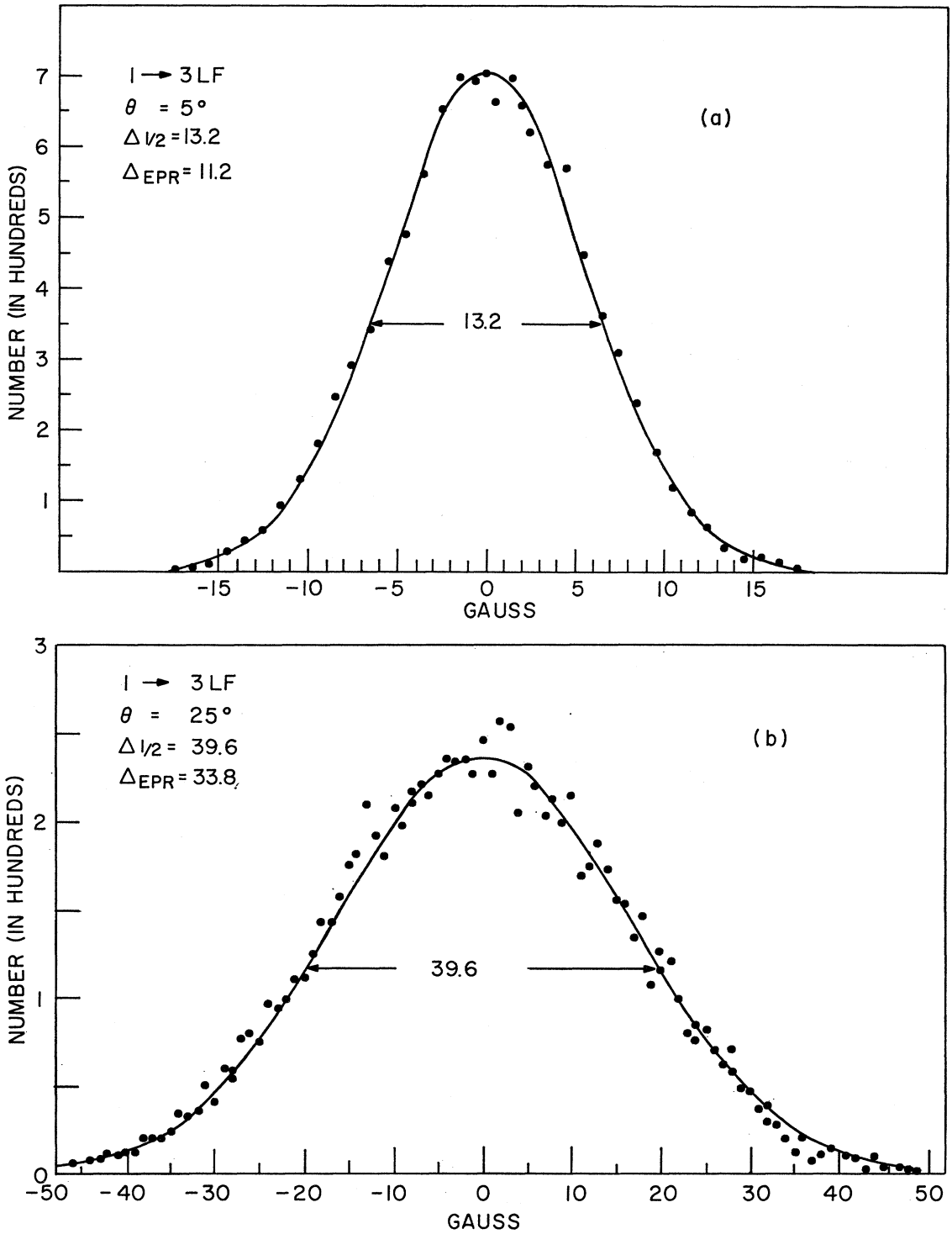

FIG. 2. EPR line shape from the Monte Carlo calculation. The line shape calculated by the Monte Carlo (statistical) method is given by the circles on figure for the (a) $\theta=5°$ $1\rightarrow 3$ *LF* transition and (b) $\theta=25°$ $1\rightarrow 3$ *LF* transition. The solid line is a superimposed Gaussian line shape. The full width at half-maximum (G) is also indicated on the figure.

with the proper frequency. If it were desirable to include temperature effects, the frequency of the choice of states could be weighted by the appropriate Boltzman factor. Once the initial state is chosen, the choice of the final state can be accomplished by generating a random number x, between 0 and 1, and comparing it

with the $P_i(j,k)$. If

$$\sum_{k=0}^{k=k_0} P_i(j,k) < x \leq \sum_{k=0}^{k=k_0+1} P_i(j,k) , \qquad (29)$$

with $P_i(j,0) \equiv 0$, then $k_i = k_0 + 1$. Thus, the final state can be chosen with the proper probability. This is done independently for all of the 13 nuclei and the ΔE calculated for this particular configuration. By repeating this calculation a sufficient number of times, the distribution of ΔE, i.e., the line shape, can be obtained.

This distribution has been calculated for each angle and transition, using a sample of 1×10^4 calculations of ΔE. Increasing the sample size by a factor of 3 has no effect on the line shape. The shape of the curve was obtained by plotting the number of samples of ΔE that fell in an interval range $E + \delta E$ as a function of E, where δE was 1 G.

Figure 2 shows the results for (a) $\theta = 5°$ and (b) $\theta = 25°$ for the $1 \rightarrow 3$ *LF* transition. The energy difference ΔE has been expressed in gauss, using Eq. (28). Also shown in the figures are superimposed Gaussian line shapes. The shape of the lines is clearly very close to Gaussian. The second moment, calculated by using Eq. (24), is identical with the second moment calculated from the full width at half-maximum for all of the lines and angles.

Thus, it appears that, at least for ruby and in the approximations employed for the calculation, the line shape is Gaussian, and the expression for the second moment given by Eq. (24) refers to a Gaussian line shape.

The over-all agreement between the width calculated from the hyperfine coefficients and the experimentally observed width reveals that the major source of the anisotropic broadening is the strong hyperfine interaction with the surrounding Al nuclei. The remaining linewidth not accounted for by the calculation (20–30%) may be due to several possible defect mechanisms. However, one significant fact that eliminates a number of these mechanisms is that the experimental line shape is found to be Gaussian for all angles and transitions. With this in mind, possible broadening sources are discussed in Secs. IV A, IV B, and IV C.

A. Mosaic Misorientation

In this defect mechanism, the crystal is viewed as a collection of microcrystals that are canted with respect to one another. Consequently, the z axis of the crystals will make a distribution of angles with the magnetic field. If the isofrequency plot is anisotropic, i.e., $dH/d\theta \neq 0$, the EPR line will be broadened by this distribution.

However, for the $1 \rightarrow 2$ and $1 \rightarrow 3$ *LF* transitions at $\theta = 0°$, and for the $1 \rightarrow 2$ and $3 \rightarrow 4$ transition at $\theta = 90°$, $dH/d\theta = 0$. Figure 1 shows a linewidth for these angles and transitions that is significantly larger than the hyperfine broadening. Thus, mosaic misorientation alone cannot account for all the additional broadening.

B. Strain and Electric-Field Broadening

Strains and electric fields are known to broaden the Cr^{3+} EPR line.[13–15] However, electric fields due to randomly-distributed trapped charges do not produce a Gaussian line shape.[16] If the linewidth were increased to account for the additional width by convoluting the Gaussian line shape with the appropriate line shape for electric field broadening (a Holtzmark distribution), the shape of the line would change significantly away from Gaussian. This is not observed. Strain fields produced by randomly-distributed point defects (which produce a Lorentzian line shape) would also change the shape of the Cr^{3+} EPR lines, and the same argument applies as in the case of electric field broadening. Thus, neither strain nor electric field effects can account for the additional broadening. Strains caused by dislocations produce a Gaussian line shape[16] and consequently could be responsible. However, the dislocation density in Czochralski and Verneuil ruby differ typically by several orders of magnitude. Both types of ruby have virtually the same observed linewidth for good samples with low Cr^{3+} concentration. Thus, dislocations are not responsible.

C. Broadening Due to Remote Nuclei

Aluminum nuclei more remote from the Cr^{3+} ion than the 13 considered will also contribute to the second moment. Their line shape will be Gaussian. When the (super) hyperfine interaction is much less than the nuclear Zeeman term, the expression for the second moment given in Eq. (26) is appropriate.

The second-moment calculation has been done for the 512 nearest neighbors, excluding the first 13, for which the sum is reported in Fig. 1. The maximum additional calculated width was 2.9 G. Since both lines will be Gaussian in shape, the widths add in rms fashion. This additional linewidth is consequently negligible for all angles. Thus, remote Al nuclei are not responsible for the broadening.

D. Calculational Approximations

Two approximations were employed in the calculation of the second moment. In the first, it was assumed that the energy levels of the Cr-Al system could be obtained as the sum of the Cr^{3+} energy and the energy of the nuclear level. The appropriateness of this approxi-

[13] P. L. Donoho, Phys. Rev. **133**, A1080 (1964).
[14] E. B. Royce and N. Bloembergen, Phys. Rev. **131**, 1912 (1963).
[15] R. F. Wenzel and Y. W. Kim, Phys. Rev. **156**, 356 (1967).
[16] A. M. Stoneham, Rev. Mod. Phys. **41**, 82 (1969).

mation was investigated by solving exactly the complete (6×4) chromium-aluminum energy-level problem and comparing this exact solution with the additive approximation. The energy differences for the transitions in question were the same to within about 1%, which is a negligible difference.

The second approximation is that the nuclear spins are uncoupled from one another. The error in assuming this would be of the order of the ratio of the nuclear magnetic moment to the Cr^{3+} magnetic moment or about $\mu_n/\mu_e=(1837)^{-1}$. Thus, the calculation of the linewidth should be reasonably accurate.

The broadening mechanisms discussed above thus inadequately explain the difference between the observed and calculated linewidth variation. In particular, strain and electric field effects, which are often mentioned in connection with broadening of the $\theta=0°$ EPR lines, do not appear to be present in good dilute Verneuil ruby.

In any case, clearly the major part of the broadening is caused by the aluminum hyperfine interaction.

V. CONCLUSIONS

The second moment of an EPR line broadened by nuclear hyperfine interaction can be obtained using Eq. (24) if the energy eigenvalues and eigenfunctions of the nuclei in the presence of the paramagnetic ion are known. The paramagnetic ion need not have a simple spin-level structure.

Applying this calculation to the Cr^{3+} ion in dilute ruby, the major part (70–80%) of the anisotropic linewidth broadening is found to be caused by strong (super) hyperfine interactions with 13 surrounding aluminum nuclei. The EPR line shape of the Cr^{3+} ion, strongly interacting with the aluminum nuclei, is calculated by a Monte Carlo method and is found to be Gaussian, in agreement with experimental results. Consequently, the calculation of the second moment is adequate to describe the line. Strains, electric field effects, dislocations, broadening by remote nuclei, and calculational approximations do not appear to account for the additional 20–30% broadening unexplained by the hyperfine mechanism.

ACKNOWLEDGMENTS

The author would like to thank Professor Yeong W. Kim, whose support and assistance made possible the preliminary work for this paper; Neal D. Wilsey, who pointed out Eq. (8); and Bruce J. Faraday for proofreading the paper.

PHYSICAL REVIEW B VOLUME 1, NUMBER 7 1 APRIL 1970

Magnetic Structure of Magnesium Chromite*

H. SHAKED,† J. M. HASTINGS, AND L. M. CORLISS
Chemistry Department, Brookhaven National Laboratory, Upton, New York 11973
(Received 6 October 1969)

The magnetic structure of the normal cubic spinel $MgCr_2O_4$ ($a_0=8.335$ Å) was investigated by means of neutron diffraction. Two distinct transitions to magnetically ordered states were found at ~16 and ~13.5°K. The reflections associated with the 16°K transition are explained by a class of noncollinear antiferromagnetic structures with a magnetic unit cell identical with the chemical cubic unit cell. The most symmetric of these high-temperature (H) structures belongs to the space group $P\bar{4}2'm'$. The H-structure reflections appeared with different intensities relative to the nuclear reflections in three samples and did not appear at all in two other samples. The low-temperature (L) reflections associated with the 13.5°K transition are explained by either of two nonequivalent noncollinear antiferromagnetic L structures which belong to space groups $P_{2b}2'2'2_1$ and $P_{2b}222$ with a magnetic unit cell $(2a_0,2a_0,a_0)$. The intensities of the L reflections relative to the intensities of the nuclear reflections varied somewhat among the five samples. It is suggested that the H and L structures represent two different phases which coexist below 13.5°K. The intensities of the magnetic reflections ($H+L$) are accounted for by a magnetic moment of about $2.2\mu_B$ per Cr^{3+}.

I. INTRODUCTION

THE compound $MgCr_2O_4$ has a normal spinel structure in which the Cr^{3+} and Mg^{2+} ions are situated at the B and A sites, respectively. Normal spinels with magnetic ions on the B sites and diamagnetic ions on the A sites make up a class of compounds which are of interest in the study of the B-B interactions. Assuming only first-neighbor interactions in an Ising model, Anderson[1] found a very large degeneracy associated with the lowest energy in this class of compounds. He also showed that this model will, in general, lead to short-range order, whereas long-range order will have to come from interactions with more distant

* Research performed under the auspices of the U. S. Atomic Energy Commission.
† On leave from Nuclear Research Center, Negev, Beer Sheva, P. O. Box 9001, Israel.

[1] P. W. Anderson, Phys. Rev. **102**, 1008 (1956).